J. Phys. B: At. Mol. Phys. **20** (1987) 325-336. Printed in the UK

On the applicability of the impulse approximation for radiative electron capture into bound and continuum states

D H Jakubaßa-Amundsen

Physik-Department, Technische Universität München, 8046 Garching, Germany

Received 24 April 1986

Abstract. A comparison between the impulse approximation (IA) and the strong-potential Born approximation (SPB) is carried out for radiative capture of a target electron into excited bound states (REC) and into continuum states (radiative ionisation, RI) of the projectile. It is found that in the vicinity of the peak in the photon spectrum, the deviations of the SPB from the IA are small but do not disappear either for excited states or for continuum states with low momentum κ_f. The contribution of RI to the forward peak is calculated for the systems $C^{6+} \to He$ and $Ne^{10+} \to He$, showing a strong skewness towards the high-energy side. For electrons with high κ_f, large deviations between SPB and IA indicate the breakdown of an atomic description.

1. Introduction

In the attempt to extend capture theories to lower collision velocities, progress has been made with the observation that the active electron is propagating off the energy shell (Macek and Shakeshaft 1980, Jakubaßa-Amundsen and Amundsen 1980), a theory which later became known as the strong-potential Born (SPB) approximation and was applied to asymmetric collision systems (Macek and Taulbjerg 1981, Macek and Alston 1982).

Assuming that the projectile charge Z_P is much larger than the target charge Z_T, electron transfer is described in terms of capture from an intermediate continuum state, with momentum $\boldsymbol{q}$, into a projectile eigenstate, mediated either by the target Coulomb field V_T (Coulomb capture) or by the radiation field (radiative capture). This capture matrix element is weighted with the momentum distribution of the initial target state. The intermediate state, which includes the coupling to the projectile field to all orders, is described by an off-shell wavefunction in the case of SPB, the difference from the energy shell being of the order of the weak field V_T. However, because of the non-uniform convergence of an off-shell function to an on-shell one, the replacement of the off-shell function by a Coulomb wave, which leads to the impulse approximation (IA, McDowell 1961), is not necessarily a small effect even if Z_T/Z_P is small (Macek and Taulbjerg 1981).

The difference in the capture cross section arising from the use of on-shell or off-shell wavefunctions, respectively, has been extensively studied in the case of Coulomb capture from the ground state of the heavier collision partner (Jakubaßa-Amundsen and Amundsen 1981, Macek and Alston 1982). The magnitude of this off-shell effect may, however, be given incorrectly through the use of additional peaking approximations; in fact, an exact calculation of both SPB and IA (where the SPB divergence has been circumvented in the spirit of Burgdörfer and Taulbjerg (1986) by means of target inner and outer screening which shifts the elastic scattering contribution off the energy shell) shows that the differences between the two theories at intermediate collision velocities are much smaller (Jakubaßa-Amundsen 1984a) than previously assumed (Macek and Taulbjerg 1981). Nevertheless, the deviations of the SPB from the impulse approximation increase at lower velocities. Recalling that the SPB has an additional dependence on the target field through the choice of the intermediate state, compared with the IA, an increase of the off-shell effects points to a growing importance of couplings to the target field.

The investigation of radiative capture instead of Coulomb capture has the great advantage that the matrix elements are much simpler, so that peaking approximations can mostly be avoided. Moreover, the additional photon degrees of freedom allow for more extensive studies of the importance of the couplings to the weak field.

For the calculation of radiative processes, the commonly used impulse approximation (Kleber and Jakubaßa 1975, Jakubaßa and Kleber 1975) has only recently been supplemented by the strong-potential Born theory (Jakubaßa-Amundsen *et al* 1984). When this theory is used, the off-shell wavefunction has to be renormalised in order to provide the correct formula for radiative recombination at zero target charge; this is in contrast to the case of Coulomb capture where the capture matrix element vanishes as $Z_T \to 0$ so that the wavefunction need not coincide with an observable scattering state. The normalisation constant has been taken as the ratio between the unrenormalised REC cross section (Gorriz *et al* 1983), in the limit $Z_T \to 0$, and the cross section for radiative recombination, which leads to a simple Z_T-independent form. It should be noted, however, that a weak Z_T dependence cannot be excluded (Alston 1985). Small differences between SPB and IA for capture to the ground state have been found in the vicinity of the peak in the photon spectrum. Scaling properties suggest that these differences should decrease and eventually disappear when the principal quantum number n of the final state goes to infinity, because an atomic theory such as the IA becomes more appropriate as the ratio between the electronic orbiting velocity Z_P/n and the projectile velocity v becomes smaller. An additional argument for this behaviour may be taken from the structure of off-shell wavefunctions: at the very large distances from which the main contribution to the capture matrix element comes in the case of highly excited states, the off-shell state approaches an on-shell one.

This question is investigated in the present paper. However, instead of calculating radiative capture into high-lying Rydberg states, continuity across the ionisation threshold means that we can consider, equivalently, radiative ionisation (RI) with ejected electrons of near-zero energy. One can then easily proceed to higher electron energies and look for possible changes in the ratio between SPB and IA.

While REC is easily distinguishable experimentally owing to its peak structure (Jakubaßa-Amundsen *et al* 1984, Anholt *et al* 1984), radiative ionisation usually contributes only to the background of photon spectra from high-energy collisions (Kienle *et al* 1973, Jakubaßa and Kleber 1975) and is thus difficult to identify. A possible exception could be the forward peak in the electron spectrum which is formed by electrons with near-zero velocity in the projectile frame. This idea has recently been investigated in the framework of a first Born calculation (Martiarena and Garibotti 1985). In the present work the contribution of RI to the forward peak is evaluated in the impulse approximation for the cases of Ne^{10+} and C^{6+} colliding with a He target. However, as in the case of capture to bound states (Briggs and Dettmann 1974, Shakeshaft 1979) radiative ionisation will dominate Coulomb capture to the continuum

(CTC) only at rather high collision velocities; this has been shown by means of an asymptotic expansion (Shakeshaft and Spruch 1978).

The paper is organised as follows. In § 2, the SPB theory for radiative electron capture is reviewed, and extended in § 3 to radiative ionisation. Numerical results are presented in § 4 and the conclusions are drawn in § 5. Atomic units ($\hbar = m = e = 1$) are used unless otherwise indicated.

2. Theory for radiative electron capture (REC)

In the independent-electron picture, the semiclassical approximation leads to the following transition amplitude for radiative capture from a bound target state ψ_i^{T} into a bound projectile state ψ_f^{P} (Kleber and Jakubaßa 1975, Jakubaßa-Amundsen *et al* 1984)

$$a_{fi} = -\mathrm{i}\int_{-\infty}^{\infty} \mathrm{d}t \int \mathrm{d}\boldsymbol{q}\langle\psi_f^{\mathrm{P}}|H_R|\psi_{\boldsymbol{q},E}^{\mathrm{P}}\rangle\langle\boldsymbol{q}|\psi_i^{\mathrm{T}}\rangle$$
$$H_R = (\mathrm{i}/c)(c^2/4\pi^2\omega)^{1/2}\,\mathrm{e}^{\mathrm{i}\omega t}\boldsymbol{u}_\lambda\boldsymbol{\nabla}_r \tag{2.1}$$

where $\psi_{\boldsymbol{q},E}^{\mathrm{P}}$ is a continuum off-shell (SPB) or on-shell (IA) projectile state with energy $E = E_f^{\mathrm{P}} + \omega$ or $q^2/2$ respectively, $|\boldsymbol{q}\rangle$ is an electronic plane wave with momentum $\boldsymbol{q}$, ω is the frequency and $\boldsymbol{u}_\lambda$ the polarisation direction of the emitted photon, and the dipole approximation of the radiation field H_R has been used. Denoting the energies of the initial and final electronic states by E_i^{T} and E_f^{P}, respectively, the differential cross section for photon emission into the solid angle $\mathrm{d}\Omega_\gamma$ is obtained by integrating $|a_{fi}|^2$ over the impact parameter (using a straight-line trajectory) and summing over $\boldsymbol{u}_\lambda$

$$\frac{\mathrm{d}\sigma}{\mathrm{d}\omega\,\mathrm{d}\Omega_\gamma} = \frac{4\pi^2\omega}{c^3 v}\sum_\lambda \int \mathrm{d}\boldsymbol{q}\,\delta(E_f^{\mathrm{P}} - E_i^{\mathrm{T}} + \omega + \boldsymbol{q}\cdot\boldsymbol{v} + v^2/2)|\varphi_i^{\mathrm{T}}(\boldsymbol{q}+\boldsymbol{v})|^2$$
$$\times|\langle\psi_f^{\mathrm{P}}(\boldsymbol{r})|\boldsymbol{u}_\lambda\boldsymbol{\nabla}_r|\psi_{\boldsymbol{q},E}^{\mathrm{P}}(\boldsymbol{r})\rangle|^2 \tag{2.2}$$

where φ_i^{T} is the Fourier transform of ψ_i^{T} and $\boldsymbol{v}$ is the collision velocity. If hydrogenic wavefunctions are used, the radiation matrix element can be found analytically for IA as well as for SPB; this is given explicitly in case of capture to the ground state in Jakubaßa-Amundsen *et al* (1984). For excited final states, the matrix element can similarly be obtained from

$$M_0 \equiv \langle\exp(-Zr)|r^{-1}\exp(\mathrm{i}\boldsymbol{s}\cdot\boldsymbol{r})|\psi_{\boldsymbol{q},E}^{\mathrm{P}}(\boldsymbol{r})\rangle$$

by means of partial derivatives with respect to Z or $\boldsymbol{s}$, where subsequently the limit $s \to 0$ has to be taken and the appropriate value for Z has to be inserted. For example, for a 3s state the matrix element is given by

$$\langle\psi_f^{\mathrm{P}}(\boldsymbol{r})|\boldsymbol{u}_\lambda\boldsymbol{\nabla}_r|\psi_{\boldsymbol{q},E}^{\mathrm{P}}(\boldsymbol{r})\rangle$$
$$= -\mathrm{i}\pi^{-1/2}Z^{3/2}\left(1 + 2Z\frac{\partial}{\partial Z} + \frac{2}{3}Z^2\frac{\partial^2}{dZ^2}\right)\lim_{s\to 0} Z\boldsymbol{u}_\lambda\frac{\partial}{\partial \boldsymbol{s}}M_0\bigg|_{Z=Z_{\mathrm{P}}/3}. \tag{2.3}$$

3. Theory for radiative ionisation (RI)

Electron capture to the continuum can likewise be calculated from (2.1), where ψ_f^{P} is replaced by $\psi_{\kappa_f}^{\mathrm{P}}$, a continuum eigenstate of the projectile with momentum κ_f. However, the radiation matrix element for RI is no longer known in closed form if an off-shell state is involved. Instead, one can resort to momentum space where the off-shell function is known in terms of an infinite series (Roberts 1985) or, more conveniently, can be found analytically from the matrix element

$$\varphi_{q,E}(p)=(2\pi)^{-3/2}\lim_{Z\to 0}\langle e^{-Zr}|e^{-ip\cdot r}|\psi^{P}_{q,E}(r)\rangle \tag{3.1}$$

which can be evaluated using the techniques of Macek and Alston (1982):

$$\begin{aligned}\varphi_{q,E}(p)=&\frac{1}{N_0}\delta(q-p)-\frac{iZ_P^2}{\pi^2\eta FD_1(B^2-C)^{1/2}N_0}\bigg\{-{}_2F_1\Big(1,1-i\eta,2-i\eta,\frac{1}{\rho_+}\Big)\\&\times\frac{1}{(1-i\eta)\rho_+}\Big(\frac{F'}{F}+\frac{2BB'-C'}{2(B^2-C)}+\frac{i\eta}{\rho_+}\rho'_+\Big)\\&+\Big[{}_2F_1(1,i\eta,1+i\eta,\rho_-)\frac{1}{i\eta}+\frac{\pi i}{\sinh\pi\eta}(-\rho_-)^{-i\eta}\Big]\\&\times\Big(\frac{F'}{F}+\frac{2BB'-C'}{2(B^2-C)}+\frac{i\eta}{\rho_-}\rho'_-\Big)-\frac{1}{\rho_+(\rho_+-1)}\rho'_+-\frac{1}{\rho_-(1-\rho_-)}\rho'_-\bigg\}.\end{aligned} \tag{3.2}$$

In this expression, ${}_2F_1$ is a hypergeometric function and the primes denote derivatives with respect to Z. The following abbreviations have been used:

$$\begin{aligned}&\eta=Z_P/K \qquad K=(2E+i\varepsilon)^{1/2}\\&D_1=-K^2+q^2 \qquad F=(Z+iK)^2+p^2 \qquad C=[(Z-iK)^2+p^2]/F\\&B=[(K^2+q^2)(K^2+Z^2+p^2)-4K^2q\cdot p]/(FD_1) \qquad \rho_\pm=B\pm(B^2-C)^{1/2}.\end{aligned} \tag{3.2a}$$

The constant $N_0=\Gamma(1+iZ_P/v)\exp(\pi Z_P/2v)$ is the renormalisation factor of the off-shell wavefunction, and the infinitesimal quantities $\varepsilon=+0$ and $Z=+0$ have been retained in order to keep track of the analytical behaviour of (3.2).

In the on-shell case, the momentum space wavefunction has the well known form (see e.g. Roberts 1985)

$$\begin{aligned}\varphi_{q,q^2/2}(p)=\varphi_q(p)=&\frac{1}{\pi^2}\exp(\pi\eta_q/2)\Gamma(1-i\eta_q)\\&\times\Big((Z_P+i\delta\eta_q)\frac{A_q^{-i\eta_q-1}}{B_q^{1-i\eta_q}}+(1-i\eta_q)\delta\frac{A_q^{-i\eta_q}}{B_q^{2-i\eta_q}}\Big)\end{aligned} \tag{3.3}$$

where $\eta_q=Z_P/q$, $A_q=p^2-(q+i\delta)^2$, $B_q=(p-q)^2+\delta^2$ and $\delta=+0$.

The differential cross section for RI in the target frame of reference is then, in analogy to (2.2), given by

$$\begin{aligned}\frac{d\sigma}{d\omega\, d\Omega_\gamma\, dE_f\, d\Omega_f}=&\frac{4\pi^2\omega k_f}{c^3v}\sum_\lambda\int dq\,\delta(\kappa_f^2/2-E_i^T+\omega+q\cdot v+v^2/2)|\varphi_i^T(q+v)|^2\\&\times\Big|\int dp\,\varphi^*_{\kappa_f}(p)(ip\cdot u_\lambda)\varphi_{q,E}(p)\Big|^2\end{aligned} \tag{3.4}$$

where $k_f=\kappa_f+v$ is the electron momentum in the target frame, $E_f=k_f^2/2$ and Ω_f is the solid angle of electron ejection.

In contrast to REC, where the differential cross section (2.2) can be readily evaluated without approximations, we resort to a peaking approximation (Kleber and Jakubaßa 1975) which has become known under the name 'transverse peaking'. It uses the fact that $\varphi_i^{\mathrm{T}}(\boldsymbol{q}+\boldsymbol{v})$ is strongly peaked at $\boldsymbol{q}_\perp = 0$, where $\hat{\boldsymbol{q}}_\perp$ denotes the plane perpendicular to $\boldsymbol{v}$, so that the radiation matrix element can be taken outside the $\boldsymbol{q}$ integral at $\boldsymbol{q} = q_z\boldsymbol{e}_z$ where $q_z = -(\kappa_f^2/2 - E_i^{\mathrm{T}} + \omega + v^2/2)/v$ is determined by the δ function. With this approximation, the differential cross section (3.4) integrated over the photon frequency and angle reduces to

$$\frac{\mathrm{d}\sigma}{\mathrm{d}E_f\,\mathrm{d}\Omega_f} = \frac{4\pi^2 k_f}{c^3 v^2}\sum_\lambda \int \mathrm{d}\Omega_\gamma \int_{-\infty}^{\infty} \mathrm{d}\omega\, \omega J_i(q_z+v) \left| \int \mathrm{d}\boldsymbol{p}\, \varphi^*_{\boldsymbol{\kappa}_f}(\boldsymbol{p})(\boldsymbol{p}\cdot\boldsymbol{u}_\lambda)\varphi_{q_z\boldsymbol{e}_z,E}(\boldsymbol{p}) \right|^2 \tag{3.5}$$

where J_i is the Compton profile of the initial target state.

If the photon is emitted into the direction ($\sin\theta_\gamma$, 0, $\cos\theta_\gamma$), the two polarisation directions can be taken such that $\boldsymbol{p}\cdot\boldsymbol{u}_1 = p\sin\vartheta_p\sin\varphi_p$ and $\boldsymbol{p}\cdot\boldsymbol{u}_2 = -p\sin\vartheta_p\cos\varphi_p\cos\theta_\gamma + p\cos\vartheta_p\sin\theta_\gamma$ where $\boldsymbol{p}$ has been expressed in spherical coordinates $(p, \vartheta_p, \varphi_p)$. By choosing the integration variable $\tilde{\varphi}_p = \varphi_p - \varphi_f$ rather than φ_p (where ϑ_f, φ_f are the angles of $\boldsymbol{k}_f$) the azimuthal integral can be carried out with the help of the formula

$$\begin{aligned} \int_0^{2\pi} \mathrm{d}\tilde{\varphi}_p \frac{1}{(\alpha - \beta\cos\tilde{\varphi}_p)^{n-\mathrm{i}\eta_f}} &= 2\pi F(n-\mathrm{i}\eta_f) \\ F(n-\mathrm{i}\eta_f) &= \frac{1}{(\alpha+\beta)^{n-\mathrm{i}\eta_f}}\, {}_2F_1\!\left(n-\mathrm{i}\eta_f, \tfrac{1}{2}, 1, \frac{2\beta}{\alpha+\beta}\right) \end{aligned} \tag{3.6}$$

where $\eta_f = Z_{\mathrm{P}}/\kappa_f$, $\alpha = p^2 + k_f^2 + v^2 - 2pk_f\cos\vartheta_p\cos\vartheta_f + 2pv\cos\vartheta_p - 2k_f v\cos\vartheta_f + \delta^2$ and $\beta = 2pk_f\sin\vartheta_p\sin\vartheta_f$.

As the integral over Ω_γ is easily carried out, the differential cross section for electron emission is therefore given by a three-fold integration which, in the case of capture from a hydrogenic 1s state, reads

$$\begin{aligned} \frac{\mathrm{d}\sigma}{\mathrm{d}E_f\,\mathrm{d}\Omega_f} &= \frac{2^{10}k_f Z_{\mathrm{T}}^5}{3c^3v^2}\frac{2\pi\eta_f}{1-\exp(-2\pi\eta_f)}\int_{-\infty}^{\infty}\mathrm{d}\omega\frac{\omega}{[(q_z+v)^2+Z_{\mathrm{T}}^2]^3} \\ &\times\Bigg((\sin^2\varphi_f + \tfrac{1}{3}\cos^2\varphi_f)\Bigg|\int_0^\infty p^3\,\mathrm{d}p\int_{-1}^{1}\mathrm{d}(\cos\vartheta_p)\sin\vartheta_p\varphi_{q_z\boldsymbol{e}_z,E}(\boldsymbol{p}) \\ &\times[(Z_{\mathrm{P}}+\mathrm{i}\delta\eta_f)A_f^{-\mathrm{i}\eta_f-1}(-F(-\mathrm{i}\eta_f)+\alpha F(1-\mathrm{i}\eta_f)) \\ &+(1-\mathrm{i}\eta_f)\delta A_f^{-\mathrm{i}\eta_f}(-F(1-\mathrm{i}\eta_f)+\alpha F(2-\mathrm{i}\eta_f))]\frac{1}{\beta}\Bigg|^2 \\ &+\tfrac{2}{3}\Bigg|\int_0^\infty p^3\,\mathrm{d}p\int_{-1}^{1}\mathrm{d}(\cos\vartheta_p)\cos\vartheta_p\varphi_{q_z\boldsymbol{e}_z,E}(\boldsymbol{p}) \\ &\times[(Z_{\mathrm{P}}+\mathrm{i}\delta\eta_f)A_f^{-\mathrm{i}\eta_f-1}F(1-\mathrm{i}\eta_f) \\ &+(1-\mathrm{i}\eta_f)\delta A_f^{-\mathrm{i}\eta_f}F(2-\mathrm{i}\eta_f)]\Bigg|^2\Bigg) \end{aligned} \tag{3.7}$$

with $A_f = p^2 - (\kappa_f + \mathrm{i}\delta)^2$, and a factor of 2 has been included to account for the two K electrons.

4. Results

Several integrable singularities appear in expression (3.7). From formulae (3.3) and (3.6) it follows that $\varphi_{\kappa_f}(\boldsymbol{p})$ becomes singular at $p=\kappa_f$ and $\alpha^2-\beta^2=0$, i.e. $\cos\vartheta_p=(k_f\cos\vartheta_f-v)/p$. In the case of the impulse approximation, there is a similar singularity in $\varphi_{q_z e_z}(\boldsymbol{p})$ at $p=|q_z|$ and $\cos\vartheta_p=-1$. For a numerical evaluation, it is convenient to split the integrals at the branch cuts and make a logarithmic variable substitution.

An additional branch cut exists in the SPB case at $F=0$, i.e. $p=K=(\kappa_f^2+2\omega)^{1/2}$. There, the different terms of the off-shell function (3.2) diverge differently, at most like $(K-p)^{-1-i\eta}$, so that it is necessary to isolate the strongest divergent term by means of analytical continuation of the hypergeometric function and to treat the singularity analytically. Note that the first-order poles of the off-shell function do not appear in the case of RI since $i\eta\neq n$ $(n=1,2\ldots)$.

Figures 1 and 2 show the ratio of the cross sections calculated within the strong-potential Born and the impulse approximation, respectively, for both processes (REC and RI) in the case of C colliding with He. The REC results are obtained from the formula (2.2) for capture into ns states $(n\leqslant 3)$ without any additional approximation, while for RI, the transverse peaked formula (3.7) is evaluated for forward emission $(\vartheta_f=0,\ k_f\geqslant v+0)$, where the φ_p integral is trivial. It can be seen that the off-shell effects are smaller at the higher collision velocity, but also that the dependence on the scaled frequency, $(\omega-\omega_{\text{peak}})/v$, where the peak energy equals $\omega_{\text{peak}}=v^2/2-E_f^{\text{P}}+E_i^{\text{T}}$, is rather similar for the bound states up to the ionisation threshold. For frequencies below the REC peak, the off-shell factor, defined as $d\sigma^{\text{SPB}}/d\sigma^{\text{IA}}$, is greater than one and quite large at small ω. It approaches unity in the peak region, and falls below one at still higher frequencies. This behaviour results from the dependence of the off-shell energy on ω: since $E=E_f^{\text{P}}+\omega$, the off-shell energy becomes equal to its on-shell value for $\omega\simeq\omega_{\text{peak}}+O(V_{\text{T}})$. As the phase factor of the off-shell function does not enter into the cross sections (2.2) or (3.7), this is sufficient for the SPB to coincide with the impulse approximation. The deviations of the off-shell factor from unity for

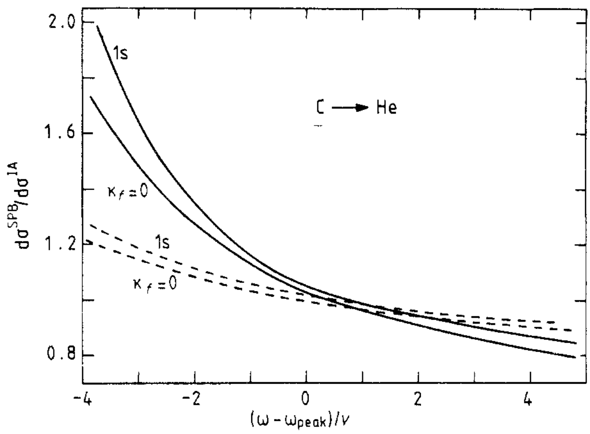

Figure 1. Ratio of the differential cross sections for radiative electron transfer between the SPB and IA theories. REC into a 1s state and RI at the ionisation threshold $(\vartheta_f=0,\ k_f=v+0)$ for photons emitted under $\theta_\gamma=90°$ are shown for the system $C^{6+}\rightarrow$ He as functions of the scaled frequency $(\omega-\omega_{\text{peak}})/v$ at $v=12$ au (full curves) and $v=20$ au (broken curves). For He, $Z_{\text{T}}=1.75$ and $E_i^{\text{T}}=-0.917\,95$ au were used.

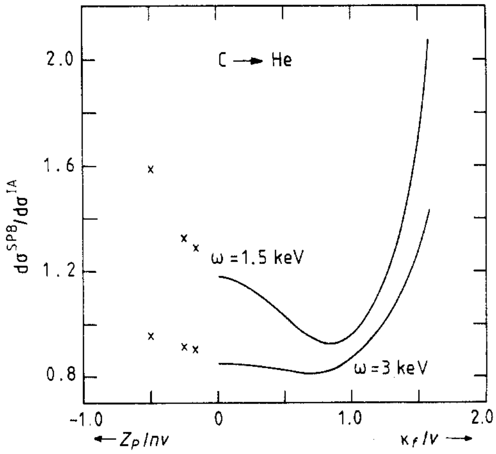

Figure 2. Ratio between the SPB and IA theory for the differential cross section for radiative electron transfer in $C^{6+} \to He$ collisions at $v = 12$ au. REC into the 1s, 2s and 3s state (×) and RI into the forward direction ($\vartheta_f = 0$, $k_f > v$) are shown as functions of the scaled electron momentum. The photons are emitted at $\theta_\gamma = 90°$ and frequencies $\omega = 1.5$ and 3 keV.

$|\omega - \omega_{\text{peak}}| \gg v$ are correlated with the large momentum transfer which is necessary to create photons with these frequencies. A large momentum transfer, however, requires small spatial distances, and it is there where on-shell and off-shell functions differ most.

In figure 2, the behaviour of the off-shell factor is displayed as a function of the reduced square root of the final-state excitation energy, $(2|E_f^{\text{P}}|)^{1/2}$ sgn E_f^{P}/v, so that the continuous passing over the threshold can be made visible. The discrepancy between the extrapolated value for $n \to \infty$ and the limit for $\kappa_f \to 0$, being less than 5%, is partly due to the peaking approximation and partly due to the fact that no angular average for radiative ionisation has been carried out. Two frequencies were chosen, one ($\omega_<$) below and one ($\omega_>$) above the K-shell peak energy (which is at 2.42 keV for this system). There is no evidence that the off-shell factor approaches unity as $n \to \infty$. Although for $\omega_<$, $d\sigma^{\text{SPB}}/d\sigma^{\text{IA}}$ decreases with n, it does not reach one at the threshold. In fact, it falls below one at low momenta κ_f of the electron, but strongly rises again when κ_f becomes larger than the collision velocity. In contrast, for $\omega_>$ the off-shell effects actually increase for higher n, while showing a similar behaviour for $\kappa_f > v$.

These results can be interpreted in terms of the interplay between the spatial characteristics of the wavefunction and the amount by which the energy is off-shell. When n becomes large, in the case of $\omega_<$ the off-shell energy increases towards its on-shell value but also larger spatial distances r of $\varphi_{q,E}^{\text{P}}$ come into play. On the other hand, for $\omega_>$, the effect of a larger r is counterbalanced by the growing off-shell to on-shell energy difference so that the deviations of the SPB from the IA are enhanced for higher n. In the case of electron ejection, the momentum of the outgoing electron plays a decisive role. While for small κ_f near threshold large distances contribute most to the radiation matrix element, when κ_f has increased beyond v there is no longer a peak frequency which corresponds to zero momentum transfer from the target electron. Instead, large momenta are required in this case so that the relevant distances become very small, as in the case of frequencies far from the peak. Also, the off-shell energy falls well below the on-shell value, giving rise to the steep increase of the ratio between the SPB and IA cross sections.

Calculations concerning the forward peak in the electron spectrum are shown in figures 3-5. As for CTC, RI also exhibits a discontinuity at $k_f = v$ and $\vartheta_f = 0$ in addition to the singular behaviour. A transformation to the projectile frame of reference reveals that this corresponds to the fact that the zero-velocity electrons are emitted with a different intensity depending on whether they are ejected at $\theta_f' = 0°$ or $\theta_f' = 180°$ relative to $\boldsymbol{v}$, a result which has already been found by Sommerfeld (1939) in the closely related bremsstrahlung theory.

Mathematically, this behaviour can be traced back to the shape of the Fourier-transformed Coulomb wave, which in the limit $\boldsymbol{k}_f = (v \pm 0)\boldsymbol{e}_z$ (i.e. $\kappa_f \to 0$) attains two different values

$$\varphi^*_{\kappa_f}(\boldsymbol{p}) \to \frac{1}{\pi^2} \exp(\pi\eta_f/2)\Gamma(1-\mathrm{i}\eta_f)\frac{1}{(p^2+\delta^2)^2} \exp\left(-\frac{2Z_\mathrm{P}}{p^2+\delta^2}(\delta \pm \mathrm{i}p \cos \vartheta_p)\right)$$
$$\times\left(Z_\mathrm{P} + \delta - \frac{2Z_\mathrm{P}}{p^2+\delta^2}(\delta \pm \mathrm{i}p \cos \vartheta_p)\right) \qquad (4.1)$$

where $\delta = +0$. This leads to an enhancement of the high-energy side of the forward peak in contrast to Coulomb capture where the low-energy side has a greater intensity. This is displayed in figure 3 where, for Ne^{10+} colliding with He, the contributions from CTC and from radiative ionisation to the forward peak are shown. For this system, experimental data are available (Berry *et al* 1985) and, for the sake of comparison, the theoretical curves (calculated in the impulse approximation) are averaged over the experimental angular and energy resolution ($\vartheta_0 = 1.4°$, $\Delta E_f = 2.2\%$) and, for RI, integrated over the photon degrees of freedom. The data can be explained by CTC, apart from the tail on the high-energy side of the peak (Jakubaßa-Amundsen 1984b). However, figure 3 makes it clear that this tail is not due to RI because, at an impact velocity of 17.62 au, though it exceeds by far the K-shell orbiting velocity of both collision partners, RI falls about two orders of magnitude below CTC.

An estimate of the relative importance of RI and CTC as a function of v is given in figure 4 for C^{6+} and Ne^{10+} projectiles on He. The number plotted there is an average

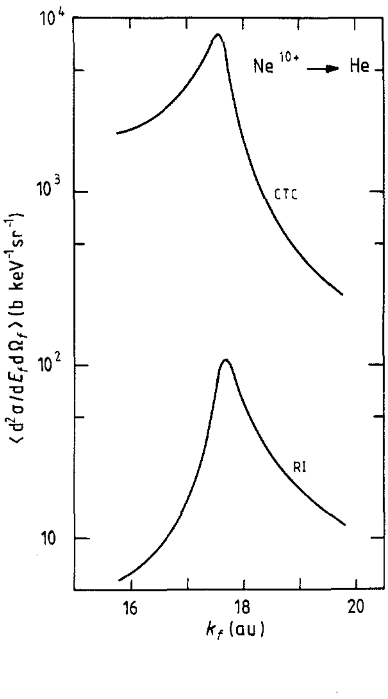

Figure 3. Angle- and energy-averaged cross section for electrons from 155 MeV Ne^{10+} on He emitted in the forward direction. The contributions to the forward peak from Coulomb capture and radiative ionisation, calculated in IA, are shown. $v =$ 17.62 au.

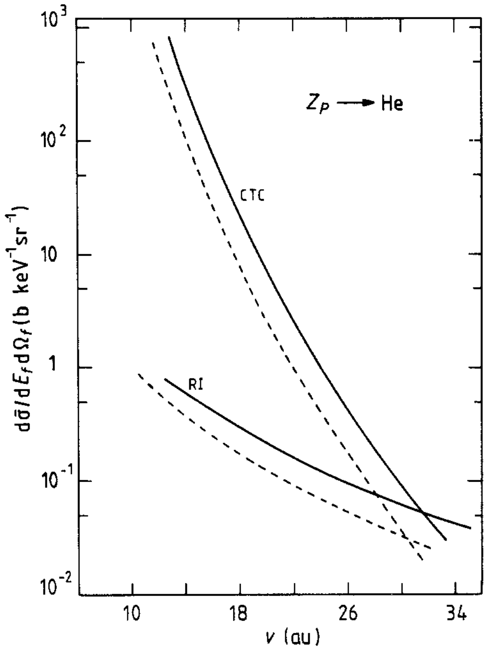

Figure 4. Differential cross section at the forward cusp as a function of collision velocity v. The results from Coulomb capture and radiative ionisation are shown for the systems Ne^{10+} on He (full curves) and C^{6+} on He (broken curves).

across the forward peak in the projectile reference frame:

$$d\bar{\sigma}/dE_f\, d\Omega_f \equiv \tfrac{1}{2}[d\sigma/dE_f\, d\Omega_f(k_f = v - \varepsilon,\ \vartheta_f = 0) + d\sigma/dE_f\, d\Omega_f(k_f = v + \varepsilon,\ \vartheta_f = 0)]/(2\pi\eta_f).$$

For CTC, numerical considerations require that $\varepsilon = Z_P/30$, whereas for RI $\varepsilon \to 0$. Owing to the slow decrease of RI with v compared with CTC, the contribution of RI becomes more and more important, dominating Coulomb capture at the still non-relativistic velocity of $v \sim 30$ au. This critical velocity is significantly higher than the value obtained from a first Born approximation ($v = 20$ au, Martiarena and Garibotti (1985)) or from an asymptotic expansion where, however, only the double-scattering term for CTC is considered ($v = 23$ au, Shakeshaft and Spruch (1978)).

In order to study the asymmetry of the forward-peak contribution from RI, the 'step number' S is defined as

$$S = \frac{d\sigma/dE_f\, d\Omega_f(k_f = v - 0)}{d\sigma/dE_f\, d\Omega_f(k_f = v + 0)} \qquad \vartheta_f = 0 \tag{4.2}$$

which is given by the cross section ratio for electron emission with $\theta_f' = 180°$ and 0°, respectively, in the projectile reference frame. This number exhibits an approximate scaling behaviour with Z_P/v (up to the order of $(Z_T/v)^2$). The scaling becomes evident if the full peaking approximation is applied to the ω-integrated cross section (3.4): $\boldsymbol{q}$ is thereby replaced by $-\boldsymbol{v}$ everywhere except in $\varphi_i^T(\boldsymbol{q}+\boldsymbol{v})$, so that both the ω and the $\boldsymbol{q}$ integrals become trivial. Together with the fact that the discontinuity will be most pronounced for values of $p \sim 2Z_P$ where the phase $(2Z_P/p)\cos\vartheta_p$ in (4.1) is close to unity, this leads to a Z_P dependence of the radiation matrix element of the form Z_P/v. This is shown in figure 5, where the step number is plotted as a function of Z_P/v. Calculations have been performed for two values of Z_P ($Z_P = 6, 10$); the results fall on a common curve with an accuracy which is in general better than 5% (which also is

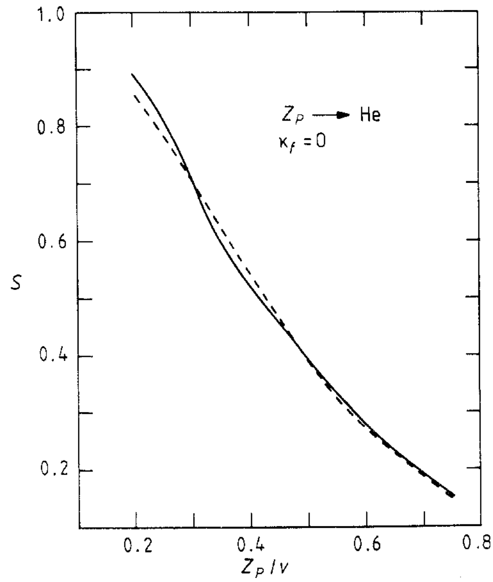

Figure 5. Step number S as a function of the scaling parameter Z_P/v. Calculations in IA (broken curve) and in SPB (full curve) are shown. The calculations were made for C^{6+} and Ne^{10+} on He; these fall roughly onto the same curve.

the numerical accuracy of the ratio S). S increases when Z_P/v becomes smaller. Its limit is $S \to 1$ for $Z_P/v \to 0$ because the discontinuity of $\varphi_{\kappa_f}(\boldsymbol{p})$ then appears only as a phase which vanishes after squaring the radiation matrix element. This high-velocity behaviour can easily be understood because, for $Z_P/v \to 0$, the intermediate state reduces to a plane wave, so that one is left with the first Born approximation where the forward peak is symmetric. The deviations of S from one may thus serve as an indication of the applicability of the first Born approximation: for a He target, Z_P/v should be less than about 0.1.

The calculations of S have been made in the impulse approximation as well as in the strong-potential Born theory. Figure 5 shows that there is a very small difference between the two theories in the whole velocity region investigated, indicating that the impulse approximation is a sufficiently accurate theory for the ω-integrated RI cross section near the ionisation threshold.

5. Conclusion

In order to study the validity of a theory for fast rearrangement collisions which is based on expansions in terms of one-centre functions (atomic theory), radiative electron transfer has been calculated within two approximations, namely the impulse approximation and the strong-potential Born theory. The latter goes beyond the IA in its consideration of the interaction of the electron with the weaker of the two nuclear potentials. It has been found that for asymmetric collisions ($Z_P \gg Z_T$) with collision velocities $v > Z_P$ the two theories give similar results in the parameter region which is relevant for integrated cross sections, i.e. for photon energies in the vicinity of the REC peak, as well as for ejected electrons with an energy below $v^2/2$. However, for photon energies well below or above the REC peak (but also for high-energy electrons), there are considerable deviations between the IA and the SPB. If it were not for the problem of the non-uniform convergence of an off-shell function to an on-shell one for Coulomb potentials, an immediate consequence of these deviations would be the necessity to include higher-order couplings to the weak field, i.e. we would need to use a molecular-type expansion for the wavefunctions. That this conclusion is nevertheless true in the present case follows from an investigation of bound-state REC, as well as δ-electron emission within a variational calculation which allows for the inclusion of molecular effects (Jakubaßa-Amundsen 1985a, b). There, it was found that for frequencies far from the REC peak as well as for high-energy electrons an atomic theory indeed becomes insufficient. The reason lies in the high momentum transfer to the active electron which in turn selects small spatial distances. When small distances become important the potentials of both nuclei have to be treated non-perturbatively. Likewise, it is at small distances where on-shell and off-shell functions differ most. So, while SPB was primarily constructed to give an improved *atomic* description, it also provides an indication of the *breakdown* of an atomic theory whenever the deviations from the impulse approximation become large.

Radiative ionisation is not only a background process, but also contributes to the forward peak in the electron spectrum. In the case of bare-projectile impact it can be neglected, compared with Coulomb capture to the continuum, for all of the collision velocities so far investigated by experimentalists; however, at a velocity of about 30 au (for impact on He), RI begins to dominate. This is interesting because CTC yields a forward peak which is skewed towards the low-energy side, while the converse is true for RI. So, when the collision velocity increases, one may expect a transition from an asymmetric peak with higher intensity on the low-energy side to a symmetric peak (where CTC and RI contribute about equally), and then back to an asymmetric one, this time with a greater intensity on the high-energy side. However, as for CTC, the asymmetry becomes weaker at the higher velocities because the step number tends to one as $Z_P/v \to 0$, with the result that it may be difficult to observe the change in the peak shape. The situation gets worse for projectiles carrying electrons because the electron loss there produces a much higher cross section. Radiative ionisation will then dominate only at much larger velocities where the cross section has probably fallen below the experimental observability.

Acknowledgments

This work has been accomplished under the watchful eyes of the youngest member of the family, R E Amundsen. I would like to thank P A Amundsen for his constant help during this project. Financial support from the GSI Darmstadt is gratefully acknowledged.

References

Alston S 1985 private communication

Anholt R, Andriamonje S A, Morenzoni E, Stoller Ch, Molitoris J D, Meyerhof W E, Bowman H, Xu J-S, Xu Z-Z, Rasmussen J O and Hoffmann D H H 1984 *Phys. Rev. Lett.* **53** 234

Berry S D, Glass G A, Sellin I A, Groeneveld K-O, Hofmann D, Andersen L H, Breinig M, Elston S B, Engar P, Schauer M M, Stolterfoht N, Schmidt-Böcking H, Nolte G and Schiewitz G 1985 *Phys. Rev.* A **31** 1392

Briggs J S and Dettmann K 1974 *Phys. Rev. Lett.* **33** 1123

Burgdörfer J and Taulbjerg K 1986 *Phys. Rev.* A **33** 2959

Gorriz M, Briggs J S and Alston S 1983 *J. Phys. B: At. Mol. Phys.* **16** L665

Jakubaßa D H and Kleber M 1975 *Z. Phys.* A **273** 29
Jakubaßa-Amundsen D H 1984a *Z. Phys.* A **316** 161
—— 1984b *Lecture Notes in Physics* vol 213, ed K-O Groeneveld, W Meckbach and A Sellin (Berlin: Springer) p 17
—— 1985a *Phys. Rev.* A **32** 2166
—— 1985b *Z. Phys.* A **320** 557
Jakubaßa-Amundsen D H and Amundsen P A 1980 *Z. Phys.* A **297** 203
—— 1981 *J. Phys. B: At. Mol. Phys.* **14** L705
Jakubaßa-Amundsen D H, Höppler R and Betz H-D 1984 *J. Phys. B: At. Mol. Phys.* **17** 3943
Kienle P, Kleber M, Povh B, Diamond R M, Stephens F S, Grosse E, Maier M R and Proetel D 1973 *Phys. Rev. Lett.* **31** 1099
Kleber M and Jakubaßa D H 1975 *Nucl. Phys.* A **252** 152
Macek J and Alston S 1982 *Phys. Rev.* A **26** 250
Macek J H and Shakeshaft R 1980 *Phys. Rev.* A **22** 1441
Macek J and Taulbjerg K 1981 *Phys. Rev. Lett.* **46** 170
Martiarena M L and Garibotti C R 1985 *Phys. Lett.* A **113** 307
McDowell M R C 1961 *Proc. R. Soc.* A **264** 277
Roberts M J 1985 *J. Phys. B: At. Mol. Phys.* **18** L707
Shakeshaft R 1979 *Phys. Rev.* A **20** 775
Shakeshaft R and Spruch L 1978 *J. Phys. B: At. Mol. Phys.* **11** L621
Sommerfeld A 1939 *Atombau und Spektrallinien* (Braunschweig: Vieweg) p 501